

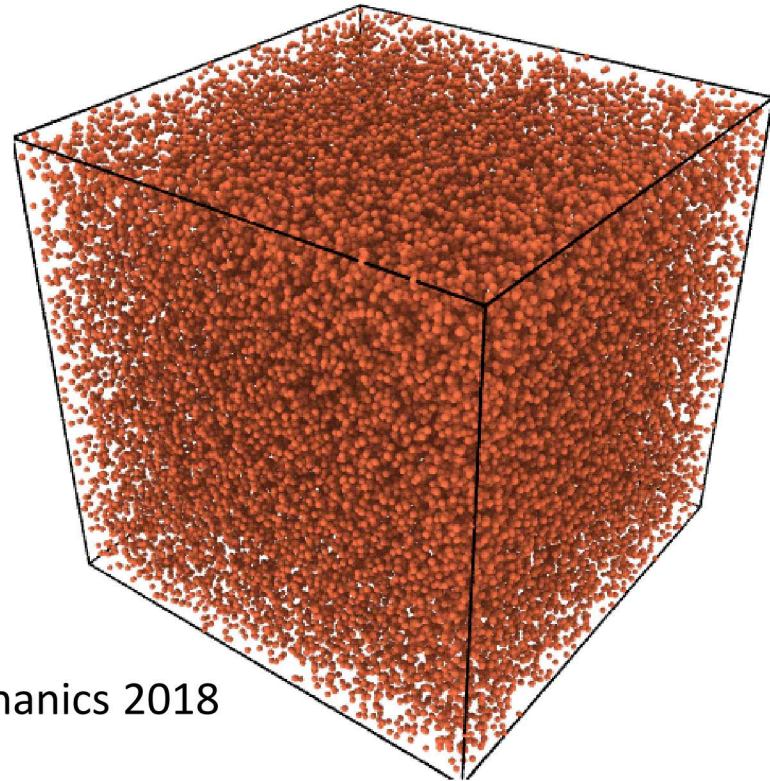
Stress-based simulations: predictions of granular flow-arrest transition and continuum rheology

Ishan Srivastava, Sandia National Laboratories

(isriva@sandia.gov)

- Leonardo E. Silbert (Southern Illinois University)
- Gary S. Grest (Sandia National Laboratories)
- Jeremy B. Lechman (Sandia National Laboratories)

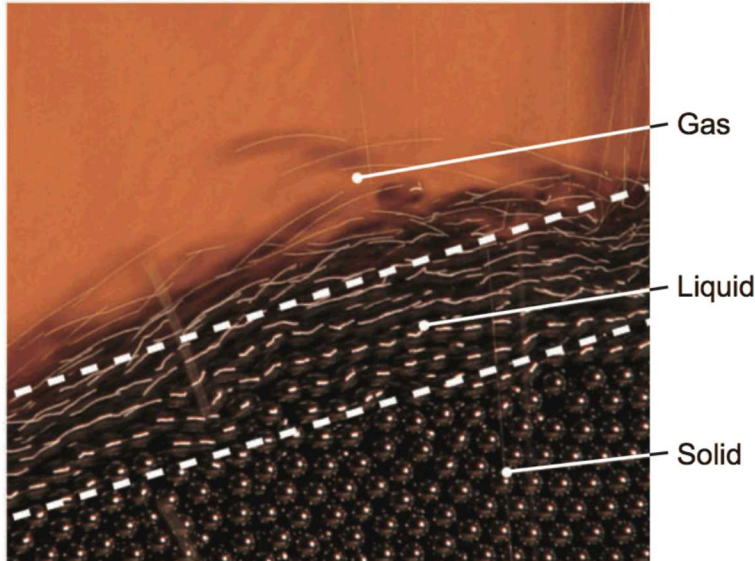
U.S. National Congress on Theoretical and Applied Mechanics 2018



Sandia National Laboratories is a multimission laboratory managed and operated by National Technology and Engineering Solutions of Sandia, LLC., a wholly owned subsidiary of Honeywell International, Inc., for the U.S. Department of Energy's National Nuclear Security Administration under contract DE-NA-0003525.

Flow Regimes in Frictional Granular Materials

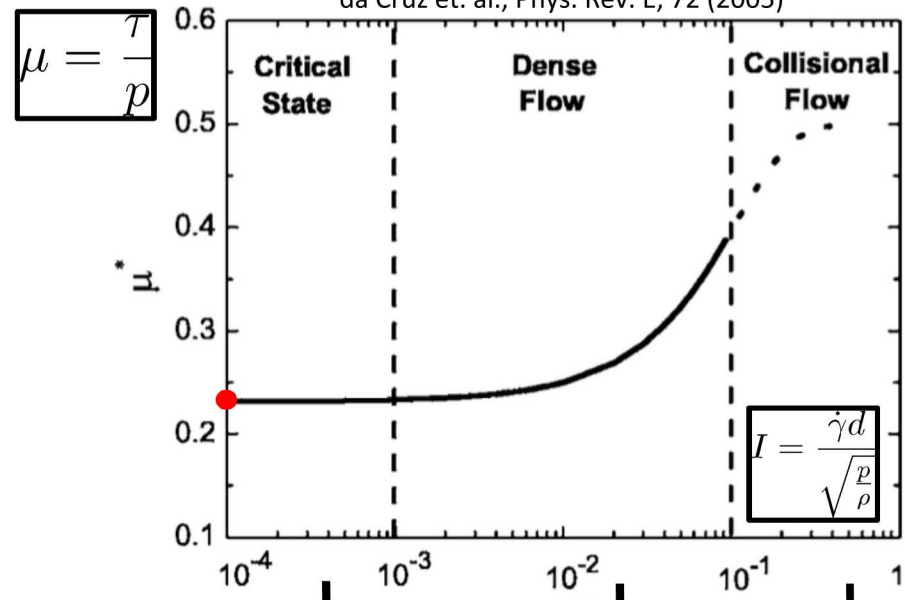
Forterre and Pouliquen, Ann. Rev. Flu. Mech., 40 (2008)



Key aspects analyzed:

- Dynamics of a granular material near the phase transition between flowing and arrest
- Three-dimensional rheology in the flowing state

da Cruz et. al., Phys. Rev. E, 72 (2005)



rate-independent
quasi-static;
yield surface concept

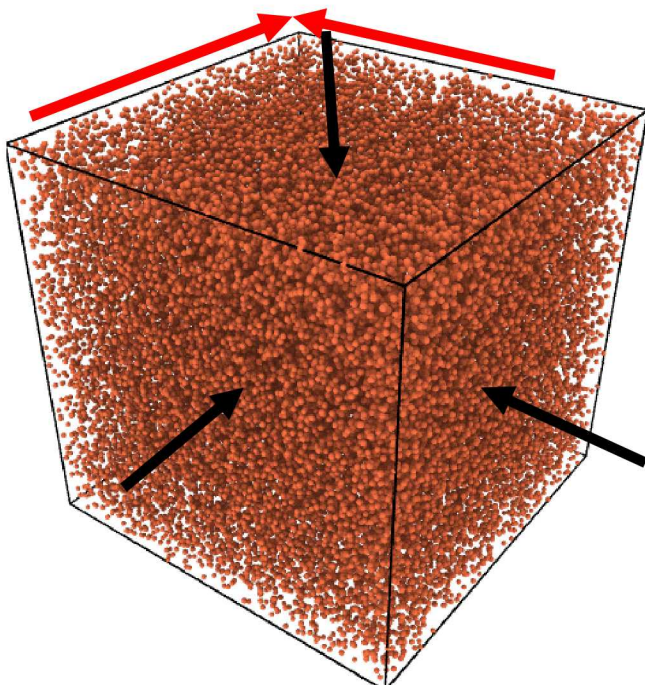
Bingham-type
visco-plastic
rheology

Bagnold
regime;
kinetic
theories

Stress Boundary Conditions: Granular RVE

second Piola-Kirchhoff stress
(thermodynamic tension)

$$\sigma_a = p_a I + \begin{bmatrix} 0 & \tau_a & 0 \\ \tau_a & 0 & 0 \\ 0 & 0 & 0 \end{bmatrix}$$



Parinello-Rahman dynamics
isenthalpic-isotension ensemble

- fully periodic with no surface effects
- uniform boundary stress state
- homogenous boundary deformation
- stable during jamming and finite-rate flows

Macroscopic Observables:

volume fraction: $\phi(t)$

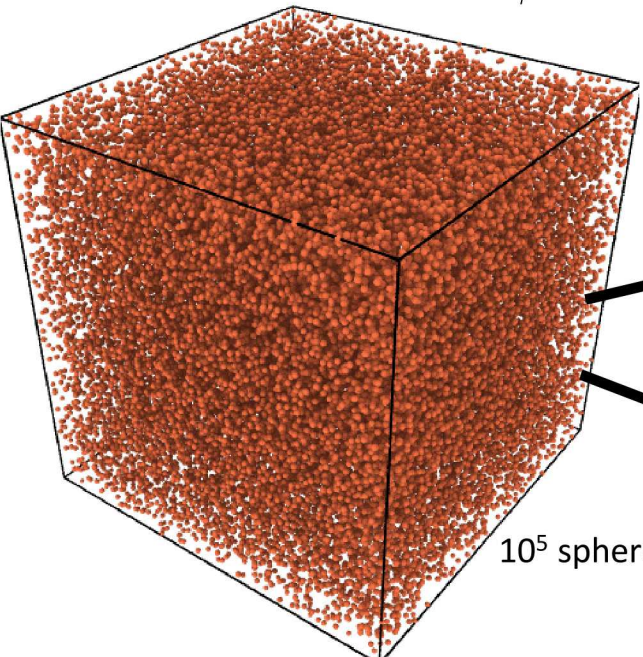
accumulated strain (3D): $\epsilon(t)$

instantaneous strain rate (3D): $\dot{\epsilon}(t)$

internal stress (3D): $\sigma(t)$

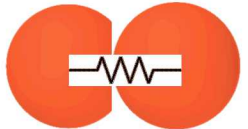
Constant Shear Stress and Pressure Simulations

initial low-density assembly: $\phi = 0.05$

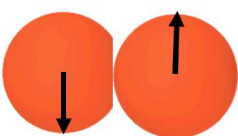


10⁵ spheres

harmonic contacts



Coulomb microscopic friction

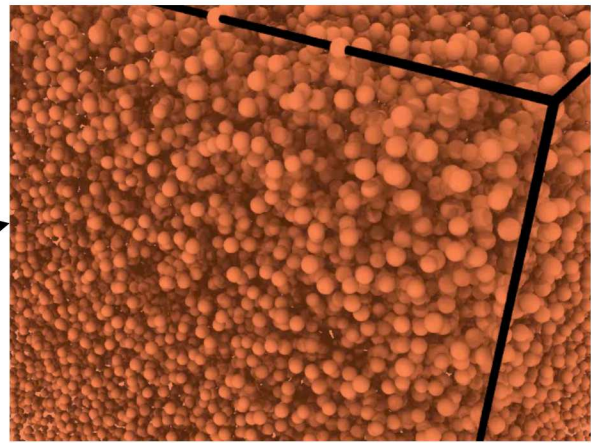


$$||F_s|| < \mu_s ||F_n||$$

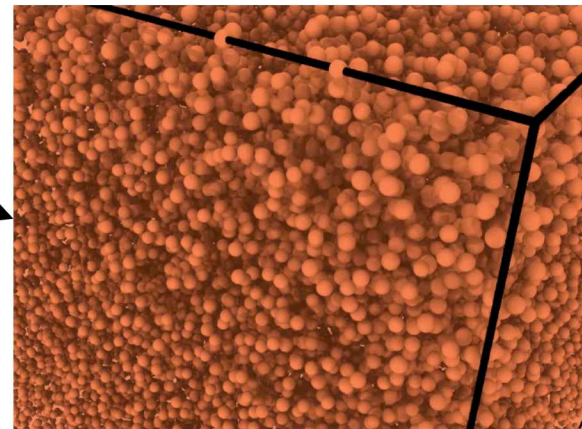
applied stress

$$\sigma_a = p_a I + \begin{bmatrix} 0 & \tau_a & 0 \\ \tau_a & 0 & 0 \\ 0 & 0 & 0 \end{bmatrix}$$

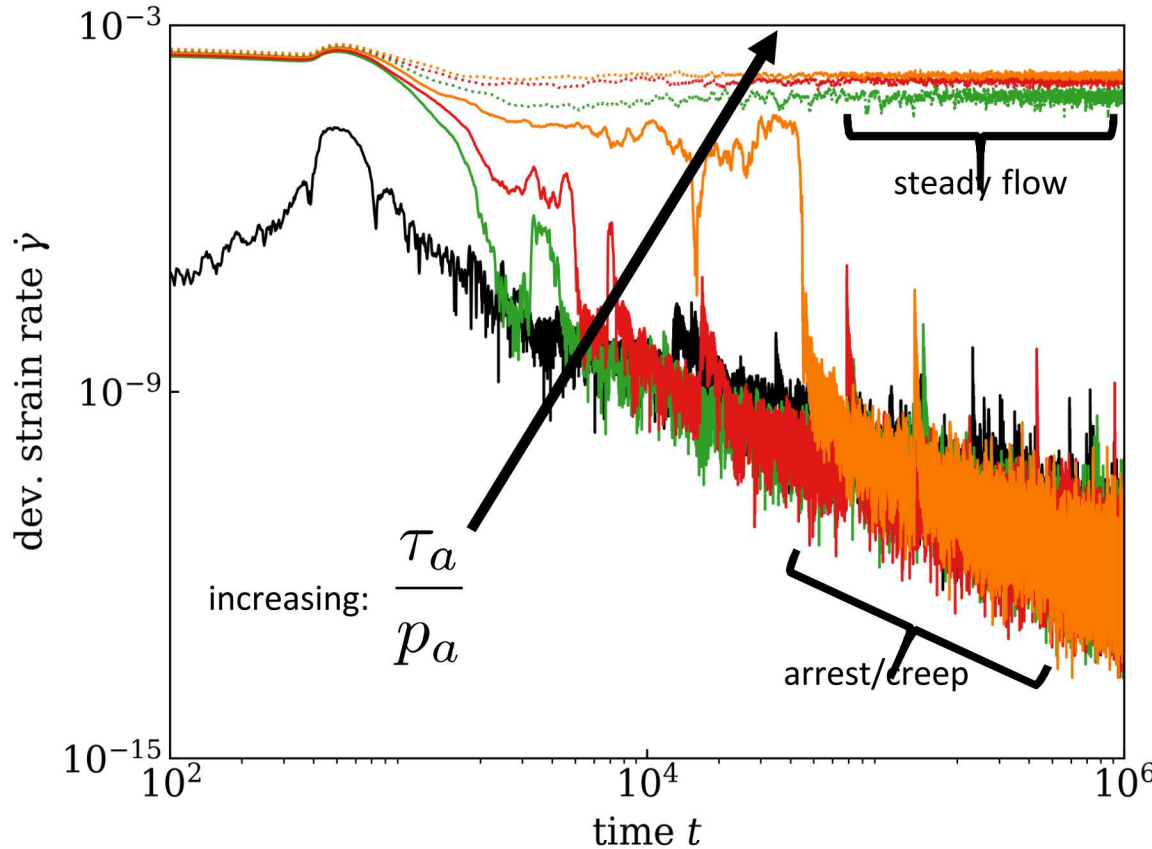
arrest



steady flow



Strain-rate Evolution: Arrest (creep) vs. Steady Flow



shear rate

$$\dot{\gamma} = \sqrt{0.5 \dot{\gamma}_{ij} \dot{\gamma}_{ij}}$$

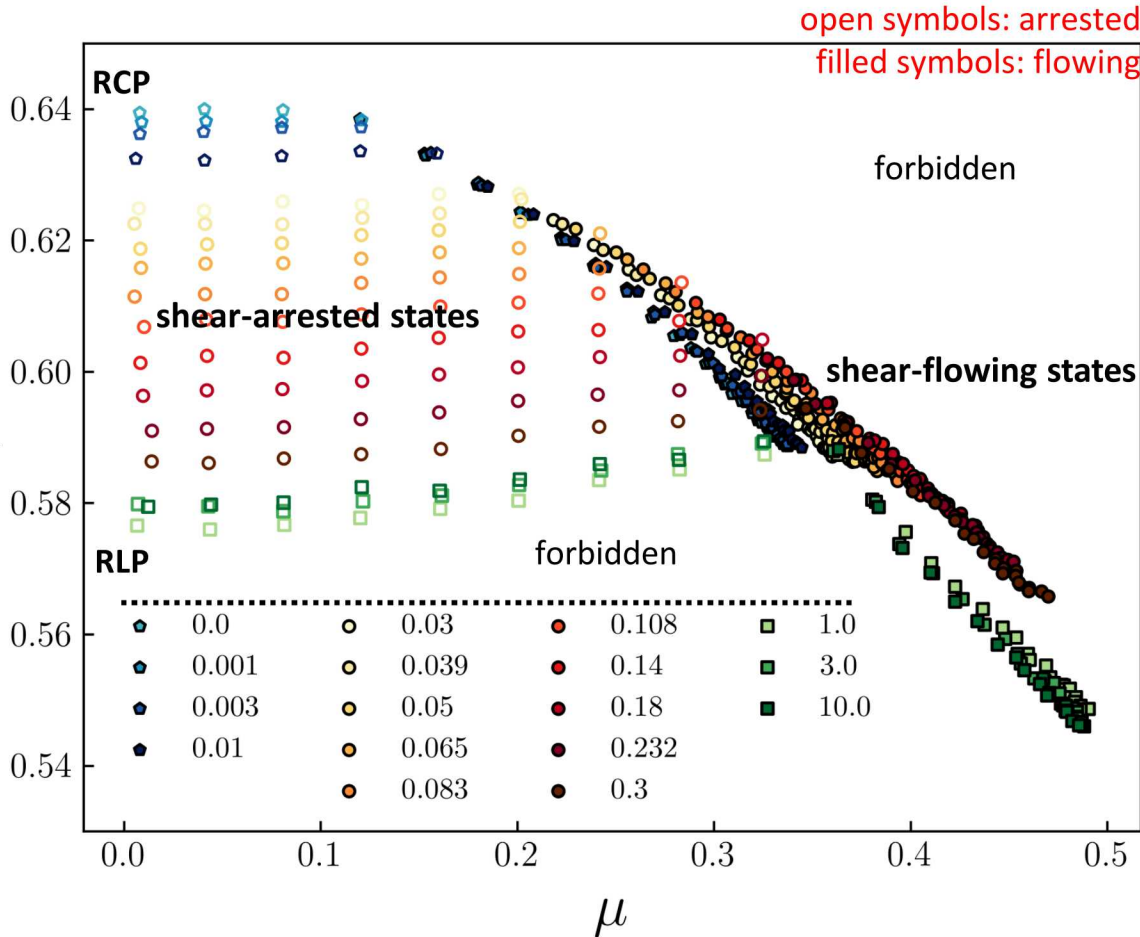
Steady Flow:

- constant strain rates at long times
- strain rate is shear stress dependent (monotonically increasing)

Arrest/Creep:

- orders of magnitude drop in strain rate during creep towards an arrested state

Steady-State Flow-Arrest Phase Diagram



$$p = \frac{1}{3} \text{tr} [\sigma] \quad \sigma_d = \sigma - pI$$

$$\mu = |\sigma_d|/p\sqrt{2}$$

Drucker-Prager

Steady Flow:

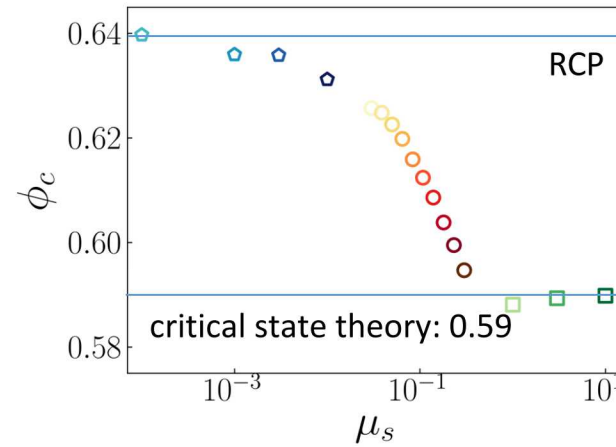
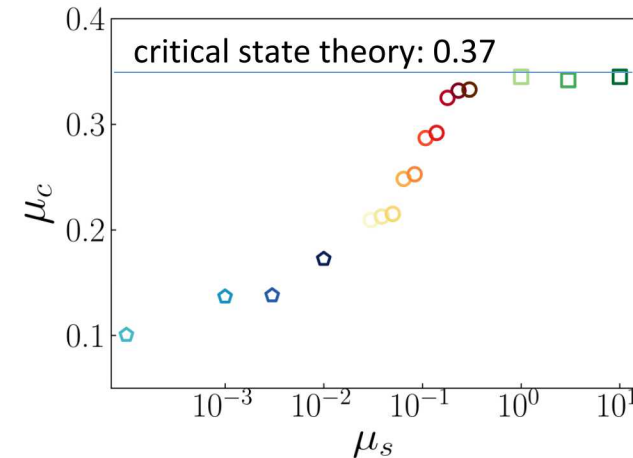
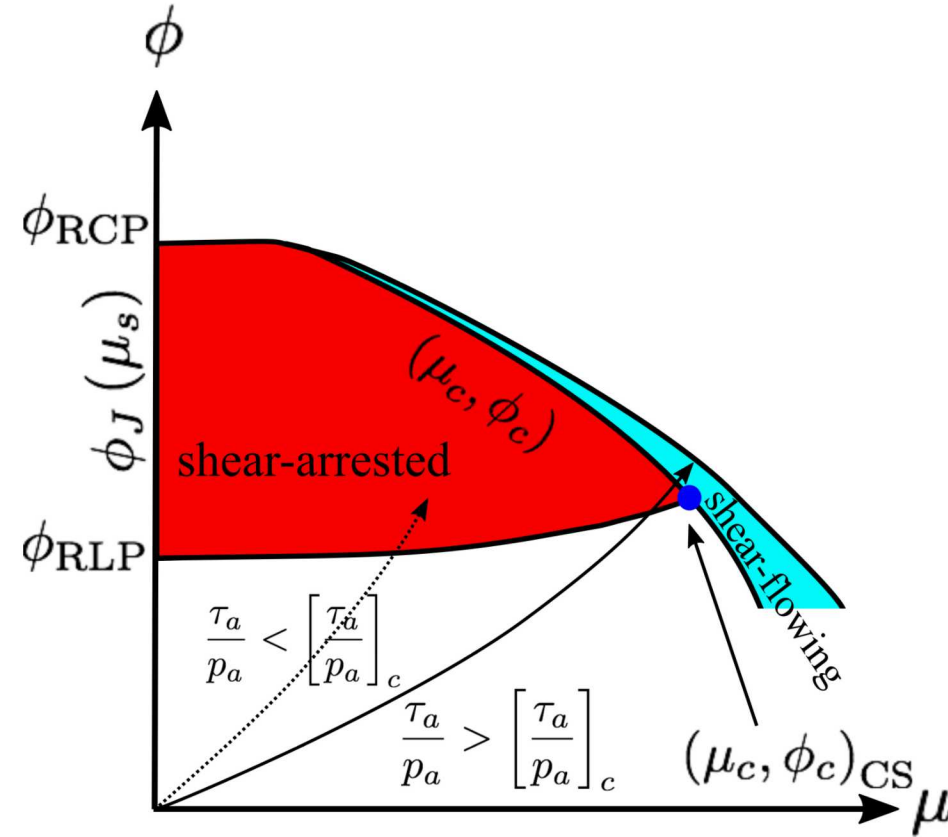
- significant **dilation** as shear stress is increased for all microscopic friction
- **static yield stress** strongly depends on microscopic friction (increases)

Arrest/Creep:

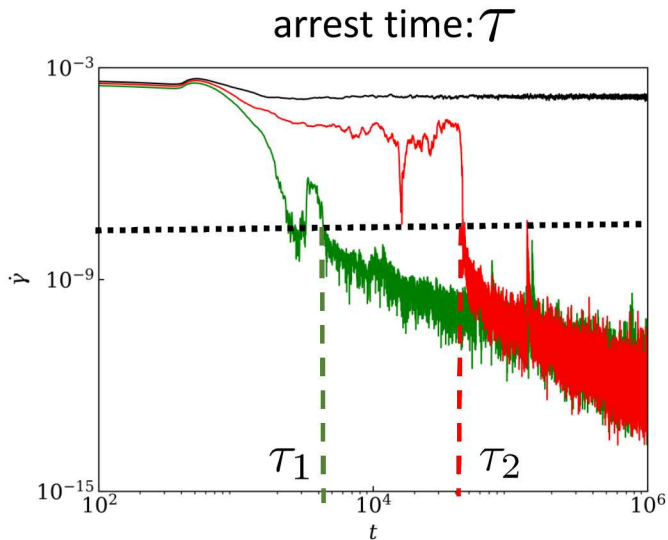
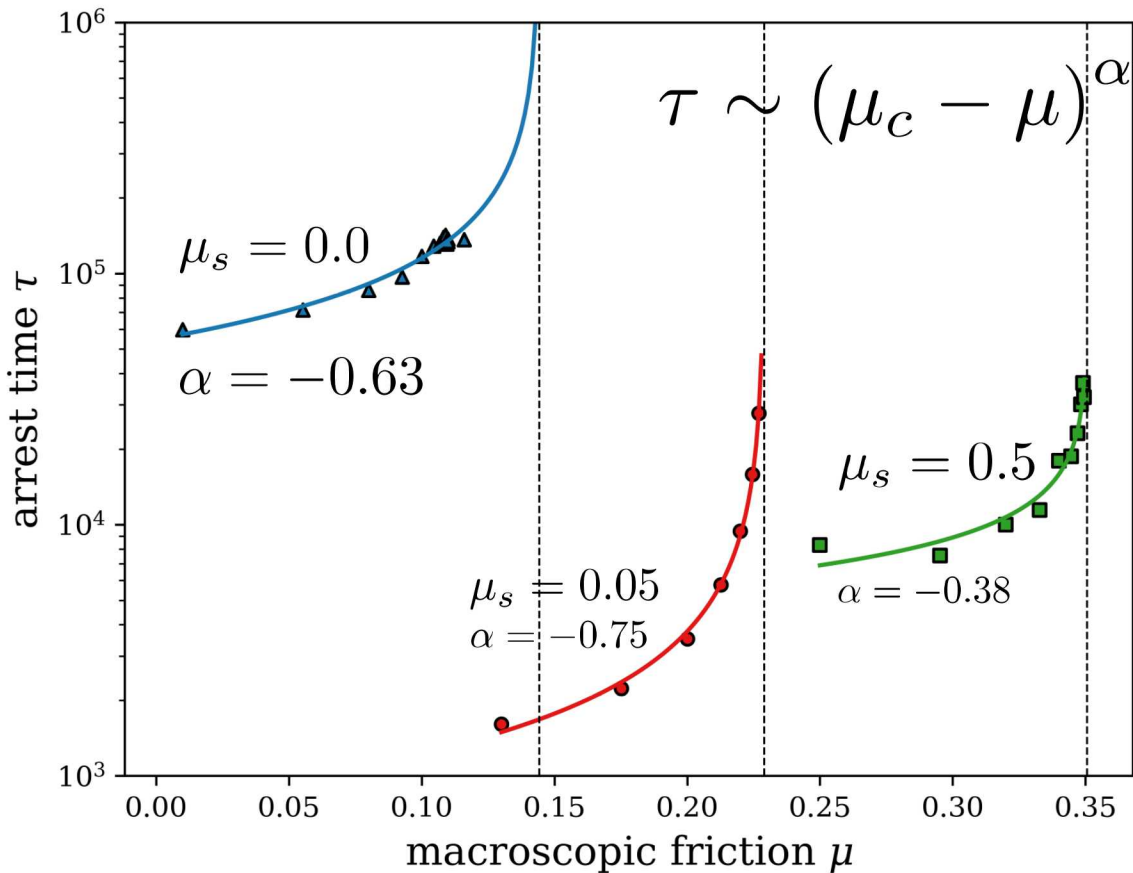
- shear-arrested states show increased **compaction** as the flow-arrest phase boundary is approached
- relative magnitude of compaction increases with increasing microscopic friction

Steady-State Flow-Arrest Phase Diagram:

Critical Points

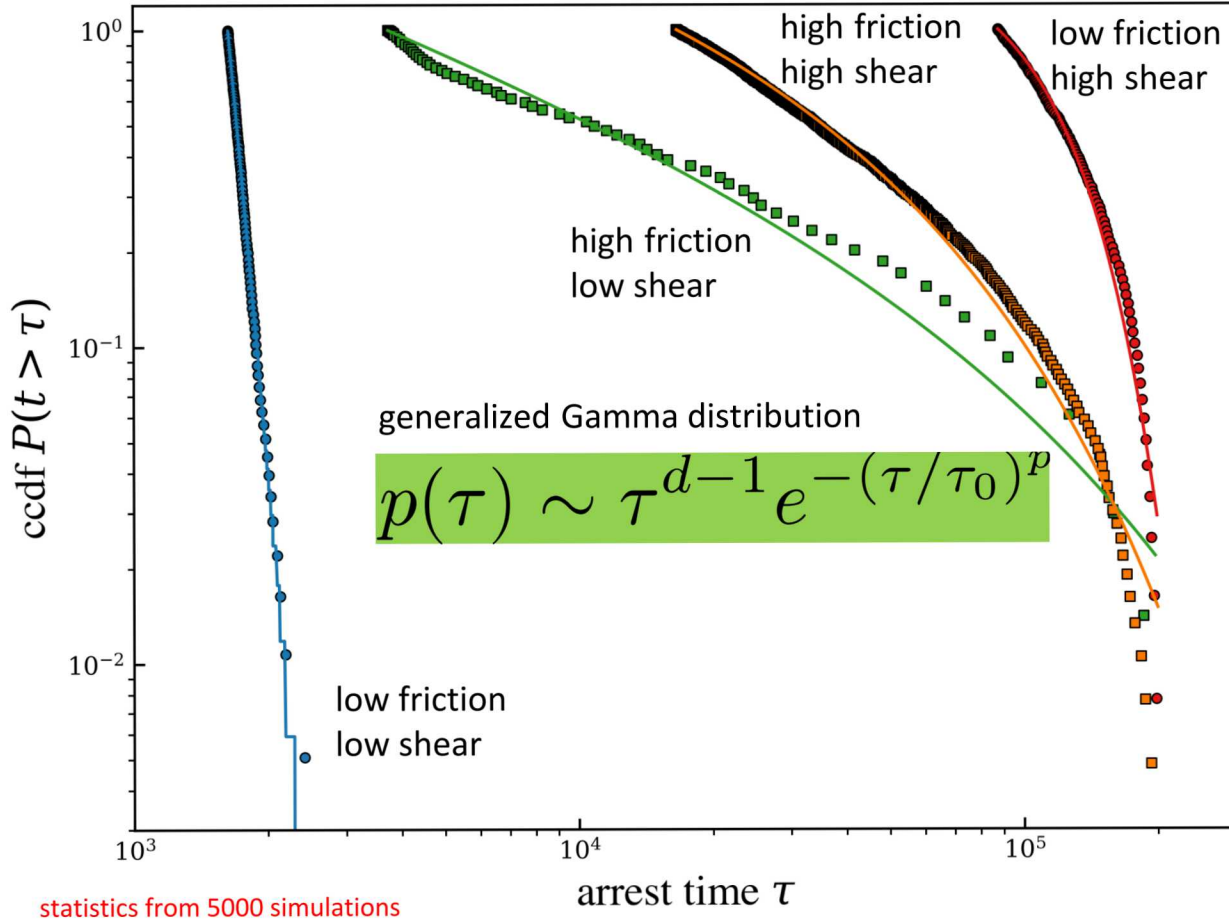


Flow-Arrest Phase Transition: Power-law Scaling



- power law scaling enables precise computation of the **critical yield stress**
- time to arrest below yield diverges at the critical yield stress as a power law
- sensitivity of the arrest time to the distance to critical yield stress increases with decreasing microscopic friction

Arrest Times Distribution



applied stress:
distance from yield stress

$$\mu_c - \mu = 10^{-3}, 10^{-1}$$

microscopic friction

$$\mu_s = 0.05, 0.5$$

- **long-tailed** distribution:
generalized Gamma distribution
- **large variance** near critical yield stress
- variance more sensitive to shear for smaller microscopic friction: could be because of increased fluctuations (noise) at particle-particle contacts (DeGiuli and Wyart, PNAS 2017)

Stress States at Yielding and Flow

$$\Delta E(t) = \int_{\Gamma} f_i \Delta u_i dS - \int_V \sigma_{ij} \frac{\partial (\Delta u_i)}{\partial x_j} dV$$


change in kinetic energy boundary traction work second order work (constitutive)

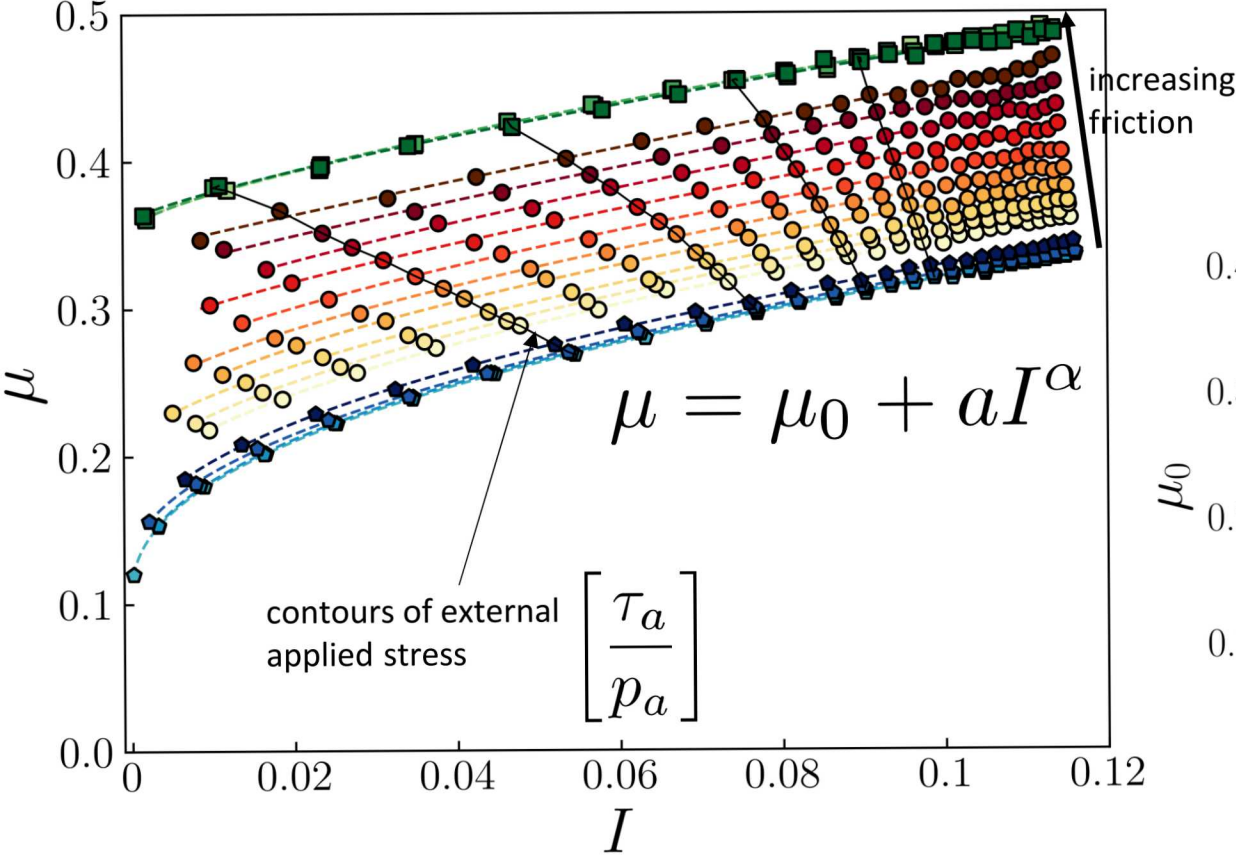
Arrest (Jammed): $\int_{\Gamma} f_i \Delta u_i dS = \int_V \sigma_{ij} \frac{\partial (\Delta u_i)}{\partial x_j} dV$

equilibrium: balance of internal and external stress

Yielding: $\int_{\Gamma} f_i \Delta u_i dS > \int_V \sigma_{ij} \frac{\partial (\Delta u_i)}{\partial x_j} dV$

rapid increase in kinetic energy: imbalance of internal and external stresses

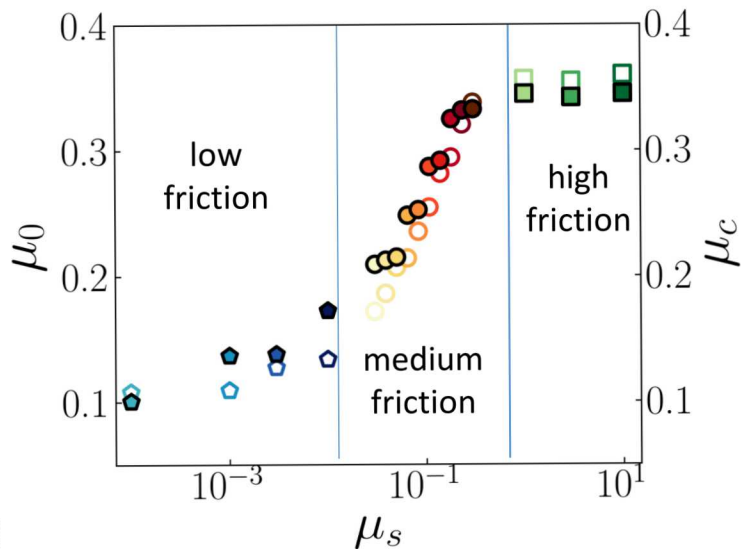
Steady State Flow: Rheology



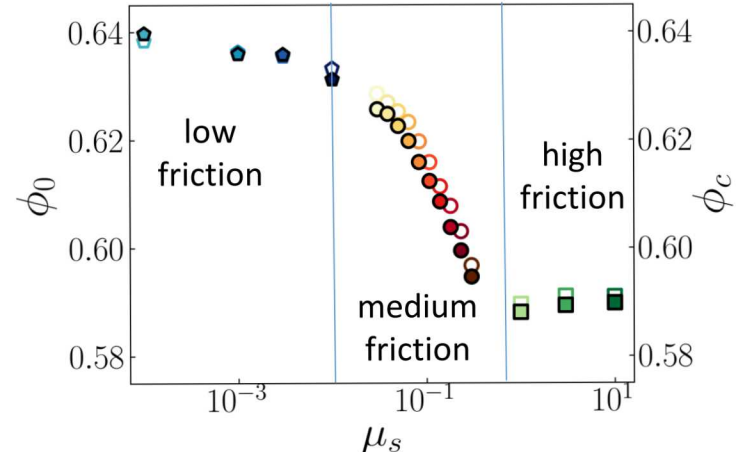
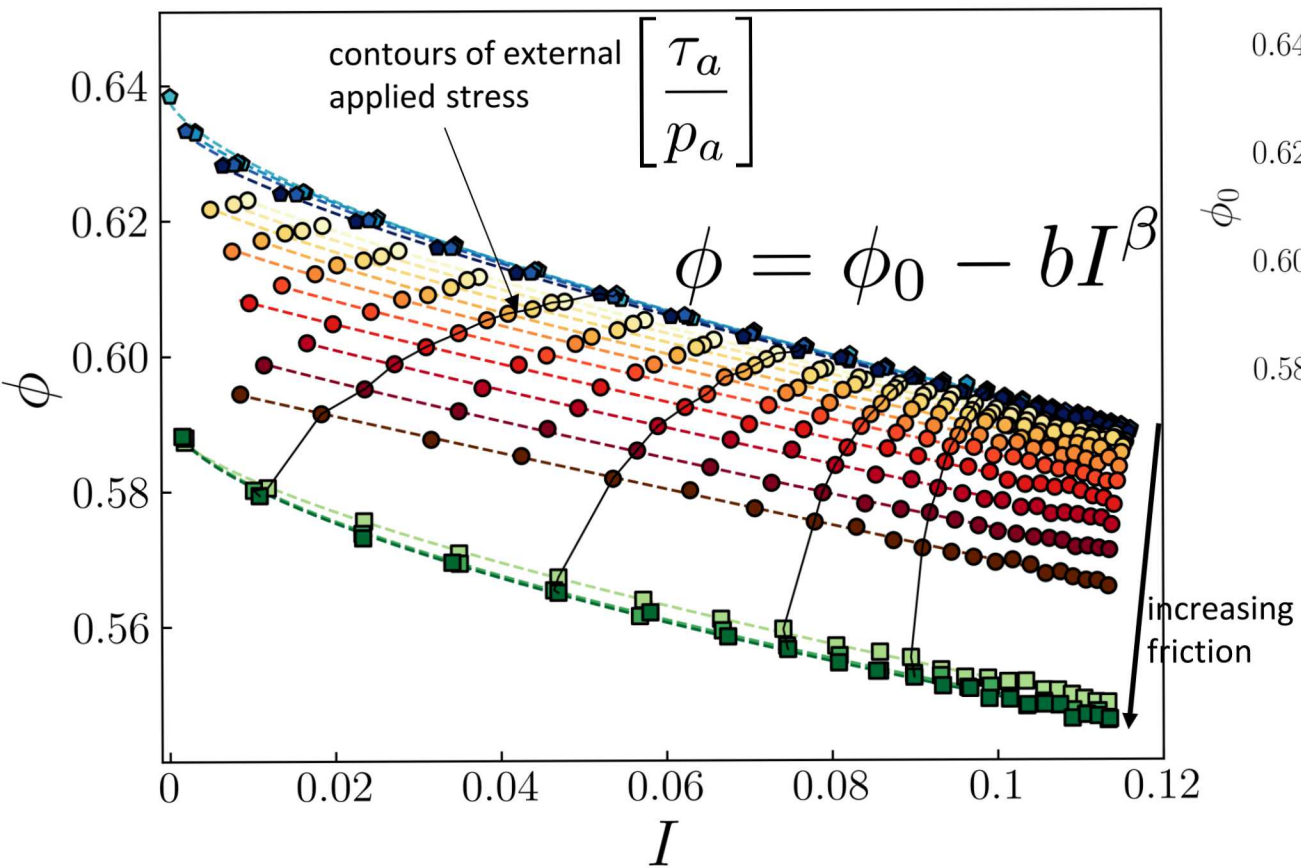
$$\mu = |\sigma_d|/p\sqrt{2}$$

$$I = |\dot{\gamma}|d/\sqrt{p/\rho}$$

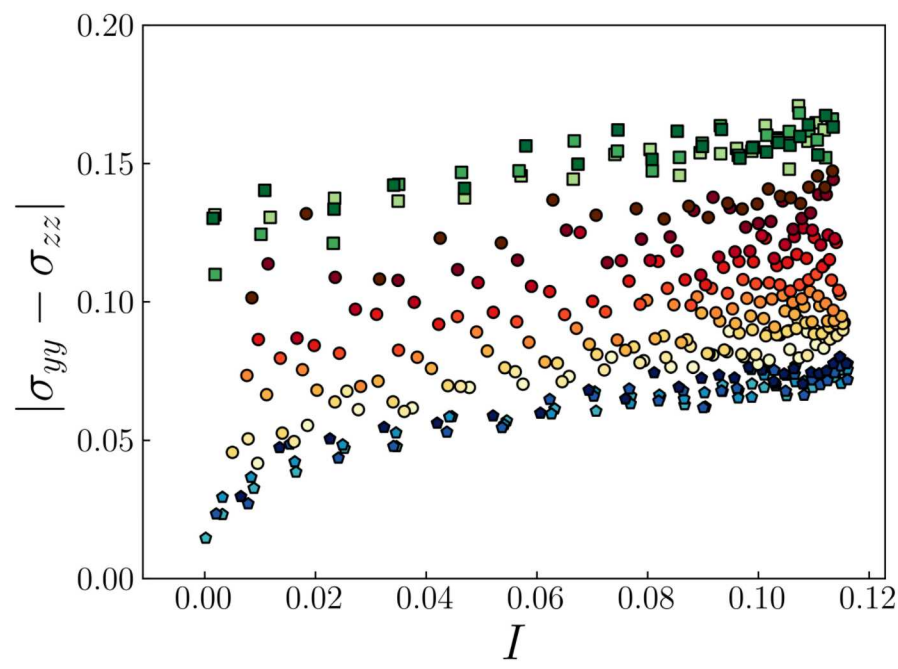
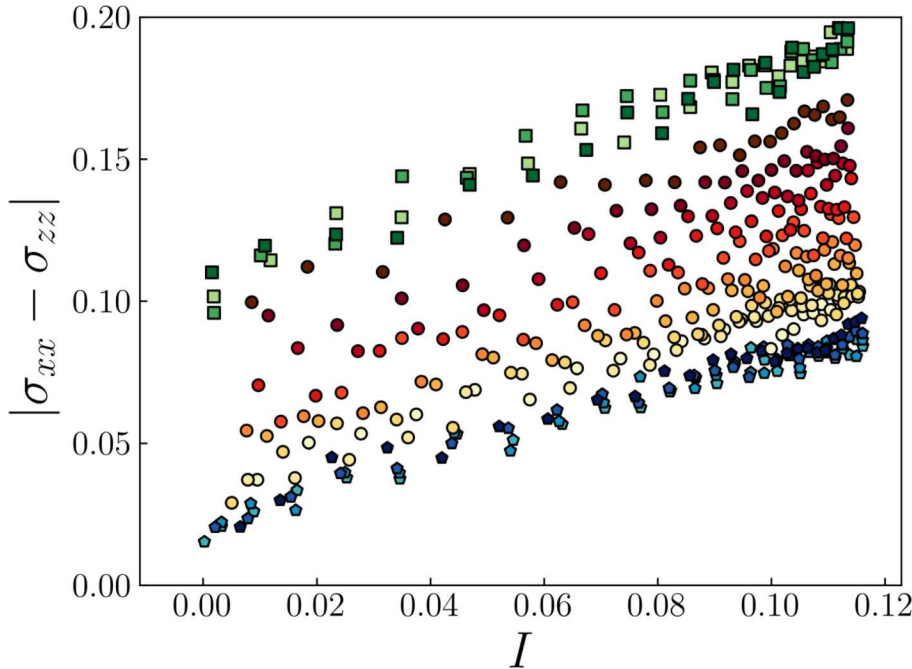
Jop et. al., Nature, 441, 2008



Steady State Flow: Dilation



Steady State Flow: Normal Stress Differences



- although granular materials dilate to flow, they're incompressible in steady state
- rheology, however, can not be described by a shear viscosity function alone
- systematic variations in the two normal stress differences are observed
- is this an example of viscometric flow characterized by viscosity and normal stress difference functions?
- need to check co-axiality/co-directionality of the flows to probe any non-viscometric behavior

Conclusions

- a homogenous stress-based method enables probing flow-arrest transition and three-dimensional granular rheology
- power-law divergence at the transition and critical phase transition line is identified; shows correspondence with known results from soil mechanics and jamming literature
- granular rheology (three-dimensional) is more complicated than predicted by $\mu(I)$ rheology; existence of normal stress difference functions indicate possibility of viscometric flows

Future Work

- subject frictional granular materials to more *complex stress loading paths* to predict 3D rheology; check for non-viscometric flows